Contribution from the Department of Chemistry,
Harvard University, Cambridge, Massachusetts 02138

A Binuclear Manganese System with Three Isolated Oxidation States: Synthesis, Structures, and Properties of Molecules with a $Mn_2(OR)_2$ Bridge Unit Containing $Mn^{III}Mn^{III}$, $Mn^{III}Mn^{II}$, and $Mn^{II}Mn^{II}$

S.-B. Yu,[1a] C.-P. Wang,[1b] E. P. Day,[1b] and R. H. Holm*,[1a]

Received March 7, 1991

The Mn(III) complex of the pentadentate ligand 2-(bis(salicylideneamino)methyl)phenolate(3–) (salmp), first prepared in 1935, has been reinvestigated in order to determine if it possesses the binuclear structure and unusual magnetic properties, and is a member of an electron-transfer series related to that, of the corresponding Fe(III) complex. The latter is part of the series $[Fe_2(salmp)_2]^{0,-,2-}$, whose preparation and properties have been recently reported. The complex $Mn_2(salmp)_2 \cdot 2MeCN$ (**1**·2MeCN) crystallizes in triclinic space group $P\bar{1}$ with a = 9.841 (2) Å, b = 10.615 (2) Å, c = 11.261 (2) Å, α = 71.00 (2)°, β = 65.58 (2)°, γ = 88.25 (2)°, and Z = 1. The molecule is composed of two *trans*-MnN_2O_4 distorted octahedra bridged by two phenolate oxygen atoms. The salmp ligand acts as a bridging and terminal ligand to each Mn atom. Reaction of **1** with 1 equiv of NaSEt in the presence of Ph_4PBr in acetonitrile affords $(Ph_4P)[Mn_2(salmp)_2]$ (**3**). The compound **3**·3.5DMF crystallizes in space group $P\bar{1}$ with a = 12.852 (2) Å, b = 13.811 (2) Å, c = 19.900 (2) Å, α = 92.84 (1)°, β = 94.92 (1)°, γ = 91.60 (1)°, and Z = 2. Reaction of **1** with 2 equiv of NaSEt in the presence of Et_4NCl in acetonitrile gives $(Et_4N)_2[Mn_2(salmp)_2]$ (**4**). The compound **4**·4MeCN was obtained in monoclinic space group $P2_1/c$ with a = 11.216 (4) Å, b = 17.445 (5) Å, c = 17.388 (5) Å, β = 104.86 (2)°, and Z = 2. The conformations of the three complexes $[Mn_2(salmp)_2]^{0,-,2-}$ are essentially identical with one another and with those in the analogous series $[Fe_2(salmp)_2]^{0,-,2-}$. These complexes are part of a five-membered electron-transfer series $[Mn_2(salmp)_2]^z$, with z = 2–, 1–, 0, 1+, and 2+; the cationic species were not isolated. $Mn_2(salmp)_2$ is centrosymmetric and exhibits a Jahn–Teller distortion, and $[Mn_2(salmp)_2]^{2-}$ is also centrosymmetric. $[Mn_2(salmp)_2]^-$ has a noncentrosymmetric, trapped-valence structure, which, from the presence of an intervalence band at 1170 nm (acetonitrile), is retained in solution. Angular distortions suggest that the structure of $[Mn_2(salmp)_2]^{2-}$ is strained by the large size of the high-spin Mn^{II} ion. The complex is sensitive to hydrolysis. The apparent yellow hydrolysis product has been separately prepared from Mn^{II}, salicylaldehyde, and a base in methanol. The compound $[Mn_2(sal)_4(MeOH)_2] \cdot MeOH$ crystallizes in space group $P2_1/c$ with a = 11.893 (3) Å, b = 20.290 (4) Å, c = 13.491 (2) Å, β = 104.14 (2)°, and Z = 4. It has an idealized centrosymmetric structure with two distorted $Mn^{II}O_6$ octahedra bridged by two phenolate oxygen atoms. Two salicylaldehyde anions are terminal ligands, and the methanol molecules are bound trans to their phenolate oxygen atoms. The ferromagnetism exhibited by the $[Fe_2(salmp)_2]^{0,-,2-}$ series is not shown by $[Mn_2(salmp)_2]^{0,-,2-}$. These complexes contain high-spin $Mn^{II,III}$ and are weakly antiferromagnetically coupled. For **1**·2DMF, J = 6.5 (2) cm^{-1} in $H_{ex} = JS_1 \cdot S_2$. The complexes $[Mn_2(salmp)_2]^{0,-,2-}$ comprise the only series in which the oxidation states $Mn^{III}Mn^{III}$, $Mn^{III}Mn^{II}$, and $Mn^{II}Mn^{II}$, supported by invariant ligands, have been structurally characterized.

Introduction

We have shown that the trianion salmp[2] is a unique binucleating pentadentate ligand that with $Fe^{III,II}$ forms centrosymmetric

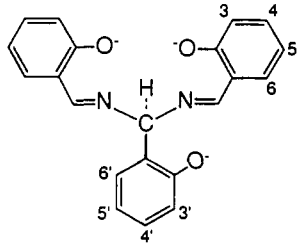

salmp

bis(ligand) complexes having doubly phenolate-bridged octahedral binding sites.[3,4] These complexes have several notable properties. (i) The three oxidation levels $[Fe_2(salmp)_2]^{0,-,2-}$, containing $Fe^{III}Fe^{III}$, $Fe^{III}Fe^{II}$, and $Fe^{II}Fe^{II}$, are stabilized and can be interconverted by chemically reversible electron-transfer reactions. (ii) All three oxidation levels have been isolated and structurally characterized. This remains the only set of binuclear iron complexes that has been structurally defined in three oxidation states. (iii) The three complexes are *ferromagnetic* rather than antiferromagnetic, as are virtually all other binuclear iron complexes in any oxidation state and bridging mode.[3,5,6] (iv) The mixed-valence complex $[Fe_2(salmp)_2]^-$ is valence-trapped below 100 K, exists at higher temperatures in an apparent equilibrium mixture of valence-trapped and valence-detrapped forms, and exhibits the rare $S = {}^9/_2$ ground state as a result of ferromagnetic coupling.[4,6]

The foregoing results raise certain issues, including the range of binuclear systems that can be formed with different metals, the stabilization of oxidation levels, and the nature and extent of magnetic coupling between metal ions. In this connection, it is interesting to note that $Fe_2(salmp)_4$ was first prepared in 1935[7] and briefly reinvestigated in 1960,[8] but its structure was incorrectly formulated at those times and the other oxidation states were not discovered. Also prepared in the early investigation[7] was a black compound formulated as "Mn(salmp)", subsequently unexamined, with the same five-coordinate structure that we have shown not to obtain with "Fe(salmp)". In view of this preparation and the current interest in polynuclear manganese compounds as possibly related to metal sites in manganese-containing proteins, a subject that has been extensively reviewed,[9-15] we have begun our investigation of the scope of metal–salmp chemistry with the

(1) (a) Harvard University. (b) Emory University.
(2) salmp = 2-(bis(salicylideneamino)methyl)phenolate(3–).
(3) Snyder, B. S.; Patterson, G. S.; Abrahamson, A. H.; Holm, R. H. *J. Am. Chem. Soc.* **1989**, *111*, 5214.
(4) Surerus, K. K.; Münck, E.; Snyder, B. S.; Holm, R. H. *J. Am. Chem. Soc.* **1989**, *111*, 5501.
(5) The great majority of such compounds are oxo- or hydroxo-bridged: Kurtz, D. M., Jr. *Chem. Rev.* **1990**, *90*, 585.
(6) All complexes with the $Fe_2(OR)_2$ bridge type are antiferromagnetic. One complex with the $Fe^{III}(OH)_3Fe^{II}$ bridge unit has been shown to be ferromagnetic with $S = {}^9/_2$: Drücke, S.; Chaudhuri, P.; Pohl, K.; Wieghardt, K.; Ding, X. Q.; Bill, E.; Sawaryn, A.; Trautwein, A. X.; Winkler, J.; Gurman, S. J. *J. Chem. Soc., Chem. Commun.* **1989**, 59.
(7) Tsumaki, T. *Bull. Chem. Soc. Jpn.* **1935**, *10*, 74.
(8) Tsumaki, T.; Antoku, S.; Shito, M. *Bull. Chem. Soc. Jpn.* **1960**, *33*, 1096.
(9) Pecoraro, V. L. *Photochem. Photobiol.* **1988**, *48*, 249.
(10) Christou, G.; Vincent, J. B. In *Metal Clusters in Proteins*; Que, L., Jr., Ed.; ACS Symposium Series 372; American Chemical Society: Washington, DC, 1988; Chapter 12.
(11) Wieghardt, K. *Angew. Chem., Int. Ed. Engl.* **1989**, *28*, 1153.
(12) Brudvig, G. W.; Crabtree, R. H. *Prog. Inorg. Chem.* **1989**, *37*, 99.
(13) Vincent, J. B.; Christou, G. *Adv. Inorg. Chem.* **1989**, *33*, 197.
(14) Christou, G. *Acc. Chem. Res.* **1989**, *22*, 328.
(15) Que, L., Jr.; True, A. E. *Prog. Inorg. Chem.* **1990**, *38*, 97.

0020-1669/91/1330-4067$02.50/0 © 1991 American Chemical Society

Table I. Crystallographic Data[a] for $Mn_2(salmp)_2 \cdot 2CH_3CN$ (**1**·2CH_3CN), $(Ph_4P)[Mn_2(salmp)_2] \cdot 3.5DMF$ (**3**·3.5DMF), $(Et_4N)_2[Mn_2(salmp)_2] \cdot 4CH_3CN$ (**4**·4CH_3CN), and $[Mn_2(sal)_4(MeOH)_2] \cdot MeOH$ (**5**·MeOH)

quantity	1·2CH_3CN	3·3.5DMF	4·4CH_3CN	5·MeOH
formula	$C_{46}H_{36}N_6O_6Mn_2$	$C_{76.5}H_{74.5}N_{7.5}O_{9.5}PMn_2$	$C_{66}H_{82}N_{10}O_6Mn_2$	$C_{31}H_{32}O_{11}Mn_2$
fw	878.8	1391.8	1221.5	690.5
a, Å	9.841 (2)	12.852 (2)	11.216 (4)	11.893 (3)
b, Å	10.615 (2)	13.811 (2)	17.445 (5)	20.290 (4)
c, Å	11.261 (2)	19.900 (2)	17.388 (5)	13.491 (2)
α, deg	71.00 (2)	92.84 (1)		
β, deg	65.58 (2)	94.92 (1)	104.86 (2)	104.14 (2)
γ, deg	88.25 (2)	91.60 (1)		
V, Å^3	1005 (1)	3513 (1)	3288 (2)	3157 (1)
Z	1	2	2	4
space group	$P\bar{1}$	$P\bar{1}$	$P2_1/c$	$P2_1/c$
ρ_{calc} (ρ_{obs}),[b] g/cm^3	1.45 (1.43)	1.32 (1.32)	1.23 (1.21)	1.45 (1.44)
T, K	297	173	297	297
μ, cm^{-1}	6.6	4.3	4.2	8.2
R^c (R_w),[d] %	4.82 (6.20)	7.58 (9.57)	5.20 (7.15)	7.17 (10.2)

[a] All data collected with Mo Kα radiation (λ = 0.71069 Å). [b] Determined by flotation in 1,4-dibromobutane/hexane. [c] $R = \sum(||F_o| - |F_c||)/\sum|F_o|$. [d] $R_w = [\sum[w(|F_o| - |F_c|)^2]/\sum[w|F_o|^2]]^{1/2}$.

manganese system. As will be seen, certain of the significant properties of the iron system can be achieved with manganese.

Experimental Section

Preparation of Compounds. All operations were carried out under a pure dinitrogen atmosphere unless otherwise noted. Et_4NCl (Fluka) was dried in vacuo at 90 °C for 24 h. Solvents were distilled and, in anaerobic preparations, were degassed prior to use.

$Mn_2(salmp)_2 \cdot 2DMF$ (1·2DMF). The preparation was adapted from the early literature[7] and was performed in the air. A solution of 6.0 g (30 mmol) of $MnCl_2 \cdot 4H_2O$ in 40 mL of water was added to a boiling solution of 15.0 g (123 mmol) of salicylaldehyde and 40 mL of 30% aqueous ammonia in 250 mL of ethanol. The yellow precipitate that formed immediately was collected by filtration and dried overnight in a vacuum desiccator. This material was oxidized by dissolving it in 200 mL of boiling chloroform; the brown solution was filtered when hot. The filtrate was allowed to stand at room temperature for 2 days, during which time black microcrystals separated. These were recrystallized from boiling DMF to afford 6.2 g (52%) of product as black crystals. Anal. Calcd for $C_{48}H_{44}Mn_2N_6O_8$: C, 61.15; H, 4.70; Mn, 11.66; N, 8.92. Found: C, 61.18; H, 4.54; Mn, 11.72; N, 8.69. Absorption spectrum (DMF): λ_{max} (ϵ_M) 332 (sh, 20200), 480 nm (sh, 4080).

$Mn_2(3\text{-}EtOsalmp)_2$ (1′). This preparation was performed in the air. A solution of 6.0 g (30 mmol) of $MnCl_2 \cdot 4H_2O$ in 40 mL of water was added to a boiling solution of 20.0 g (120 mmol) of 3-ethoxysalicylaldehyde (Aldrich) and 60 mL of 30% aqueous ammonia in 250 mL of ethanol. The mixture was boiled in a water bath for 4 h, during which ethanol was added to maintain the initial volume. A golden brown microcrystalline solid precipitated upon maintaining the reaction mixture at −20 °C overnight. This material was dissolved in boiling acetonitrile; the solution was filtered while hot. The filtrate was maintained at −20 °C overnight to give 5.8 g (36%) of product as a black-brown crystalline solid. Anal. Calcd for $C_{54}H_{54}Mn_2N_4O_{12}$: C, 61.14; H, 5.13; Mn, 10.36; N, 5.28. Found: C, 60.30; H, 4.79; Mn, 11.10; N, 5.02. Absorption spectrum (DMF): λ_{max} (ϵ_M) 332 nm (16200).

$(Et_4N)[Mn_2(salmp)_2]$ (2). A mixture of 2.0 g (2.5 mmol) of 1·2DMF, 0.21 g (2.5) mmol of NaSEt, and 0.43 g (2.6 mmol) of Et_4NCl in 100 mL of acetonitrile was stirred overnight. The red-brown reaction mixture was filtered, and the volume of the filtrate was reduced to half in vacuo. Ether was added to cloudiness, and the mixture was stored at −20 °C overnight. A brown-black crystalline solid was collected, washed with ether, and recrystallized from acetonitrile/ether (with overnight standing at −20 °C) to give 1.8 g (76%) of product. Anal. Calcd for $C_{50}H_{50}Mn_2N_5O_6$: C, 64.79; H, 5.44; Mn, 11.86; N, 7.56. Found: C, 64.42; H, 5.33; Mn, 11.45; N, 8.17. Absorption spectrum (MeCN): λ_{max} (ϵ_M) 375 (20800), 480 (sh, 2680), 1170 nm (270).

$(Ph_4P)[Mn_2(salmp)_2]$ (3). This compound was prepared by the same method and on the same scale as **2**, but with use of Ph_4PBr, and was obtained in 72% yield as a brown-black crystalline solid.

$(Et_4N)_2[Mn_2(salmp)_2]$ (4). A mixture of 2.0 g (2.5 mmol) of 1·2DMF, 0.43 g (5.1 mmol) of NaSEt, and 0.87 g (5.3 mmol) of Et_4NCl in 100 mL of acetonitrile was stirred overnight. The yellow reaction mixture was filtered, and the filtrate was taken to dryness in vacuo. The yellowish residue was dissolved in a minimal quantity of acetonitrile. Ether was allowed to diffuse into this solution, causing the separation of chunky orange crystals. These were collected and washed with ether to afford 1.1 g (42%) of product. This compound is highly sensitive to water and readily hydrolyses to compound **5**. It was dried in vacuo for 1 day prior to analysis. Anal. Calcd for $C_{58}H_{70}Mn_2N_6O_6$: C, 65.90; H, 6.67; Mn, 10.39; N, 7.95. Found: C, 66.42; H, 7.04; Mn, 9.68; N, 7.78. Absorption spectrum (MeCN): λ_{max} (ϵ_M) 303 (sh, 9250), 381 (29600), 485 nm (sh, 430).

$Mn_2(sal)_4(MeOH)_2$ (5). A solution of 2.6 g (21 mmol) of salicylaldehyde and 2.2 g (22 mmol) of Et_3N in 50 mL of methanol was added to a stirred solution of 2.0 g (10 mmol) of $MnCl_2 \cdot 4H_2O$ in 100 mL of methanol. A yellow-orange solution was obtained, which after 1 h was filtered. The volume of the filtrate was reduced in vacuo to half, causing the precipitation of some yellow microcrystalline solid. Maintenance of the mixture at −20 °C overnight followed by filtration and recrystallization of the solid from methanol yielded 2.35 g (71%) of product as yellow microcrystals. Anal. Calcd for $C_{30}H_{28}Mn_2O_{10}$: C, 54.72; H, 4.29; Mn, 16.69. Found: C, 54.74; H, 4.19; Mn, 16.80. Absorption spectrum (DMF): λ_{max} (ϵ_M) 323 (sh, 7040), 378 nm (14700).

X-ray Structural Determinations. Diffraction-quality crystals were obtained as follows: 1·2MeCN, black, irregularly shaped crystals by the slow oxidation of a dilute solution of **4** in acetonitrile; 3·3.5DMF, brown blocklike crystals by slow cooling of a concentrated DMF solution of **3**; 4·4MeCN, orange blocklike crystals by diffusion of ether into a concentrated acetonitrile solution of **4** at room temperature; 5·MeOH, yellow blocklike crystals from a methanol solution of **5** kept at −20 °C for several days. Crystals were mounted in glass capillaries and sealed under dinitrogen. Data collections were performed by using a Nicolet P3F diffractometer equipped with a Mo X-ray source and a graphite monochromator. The data collection for 3·3.5DMF was performed at 173 K; all others were carried out at room temperature. Orientation matrices and unit cell parameters were determined by least-squares fits of the angular coordinates of 50 machine-centered reflections having $20° \le 2\theta \le 30°$. Crystal data are included in Table I. Three check reflections monitored every 97 reflections indicated various extents of decay, which for 5·MeOH required correction. Lorentz and polarization corrections were applied with XDISK from the SHELXTL program package, and empirical absorption corrections were made with XEMP. Atom scattering factors were taken from a standard source.[16]

In all cases the choice of space group was confirmed by successful solution and refinement of the structure. Metal atoms in 1·2MeCN and 3·3.5DMF were located by the Patterson method with CRYSTALS and SHELXTL, respectively. In the two other compounds metal and coordinating atoms were located by using direct methods. The remaining non-hydrogen atoms in all compounds were found by successive Fourier maps and were refined by using CRYSTALS (1·2MeCN, 4·4MeCN, 5·MeOH) or SHELXTL (3·3.5DMF). All such atoms were refined anisotropically except those of disordered groups and some of the solvent molecules. In 3·3.5DMF, the half-DMF solvate molecule was severely disordered and was modeled with site occupancies of 0.5 O, 0.5 N, and two 0.75 C atoms. In the final stages of the refinements, hydrogen atoms of nondisordered groups were introduced at 0.96 Å from bonded carbon atoms. In the final refinement cycles, all parameters shifted by <1% of their esd's. The highest residual peaks in the final difference maps ranged from 0.5 (1·2MeCN) to 2.0 e/Å^3 and were located in the vicinity of the disordered groups or Mn atoms. Final agreement factors are given in Table I; positional parameters are listed in Tables II–V.[17]

(16) Cromer, D. T.; Waber, J. T. *International Tables for X-Ray Crystallography*; Kynoch Press: Birmingham, England, 1974.

Table II. Positional Parameters ($\times 10^4$) for $Mn_2(salmp)_2 \cdot 2CH_3CN$ ($1 \cdot 2CH_3CN$)

atom	x/a	y/b	z/c
Mn(1)	760.1 (7)	1473.4 (6)	4173.2 (7)
O(1)	1230 (3)	2792 (3)	2338 (3)
O(2)	2000 (3)	2449 (3)	4519 (3)
O(3)	570 (3)	-335 (3)	5977 (3)
N(1)	2531 (3)	402 (3)	3101 (3)
N(2)	-1139 (3)	1796 (3)	5742 (3)
C(1)	-3537 (4)	-961 (4)	8148 (4)
C(2)	1114 (4)	-2579 (4)	3618 (4)
C(3)	2622 (4)	-1021 (4)	3806 (4)
C(11)	-3655 (5)	-2301 (5)	9064 (5)
C(12)	-2488 (5)	-3144 (4)	8794 (4)
C(13)	-2701 (6)	-4393 (5)	9847 (5)
C(14)	-3986 (7)	-4789 (6)	11062 (6)
C(15)	-5121 (7)	-3965 (6)	11310 (6)
C(16)	-4950 (6)	-2751 (5)	10332 (5)
C(21)	-198 (4)	-3381 (4)	3857 (4)
C(22)	-1673 (4)	-3281 (4)	4772 (4)
C(23)	-2876 (5)	-4095 (4)	4903 (5)
C(24)	-2624 (5)	-4959 (5)	4182 (6)
C(25)	-1173 (6)	-5085 (5)	3295 (6)
C(26)	18 (5)	-4287 (5)	3138 (5)
C(31)	2903 (4)	-1165 (4)	5046 (4)
C(32)	1808 (4)	-827 (4)	6129 (4)
C(33)	1981 (5)	-986 (5)	7326 (5)
C(34)	3274 (5)	-1449 (5)	7433 (5)
C(35)	4382 (5)	-1760 (4)	6353 (5)
C(36)	4198 (4)	-1629 (4)	5170 (5)

Magnetic Measurements. These were performed and the data were fit as in earlier work,[18] except that the finely ground powder sample of **1**·2DMF was held in place physically between the gel cap halves without adding mineral oil. No detectable ferromagnetic impurities were seen in the gel caps used. Magnetization curves were calculated as previously described.[19] The major ambiguity in the analysis of the magnetic data (Figure 5) is in the level of paramagnetic impurities. The final fit of the data was obtained by first finding the best possible fit ($\chi^2 = 11$) to the raw data by assuming zero impurity. Then a trial amount (<0.5%) of monomeric $S = 2$ Mn^{III} impurity having magnetic properties identical with those of the Mn^{III} sites in the sample was subtracted from the raw data, causing an improved fit. This process was repeated until the best fit was obtained ($\chi^2 = 3.7$ with 0.37% impurity subtracted). In this iterative process, the amount of pure sample measured changed in successive fits. The uncertainties in the spin Hamiltonian parameters reported (vide infra) reflect the changes in these parameters observed during this iterative search for the appropriate impurity level.

Other Physical Measurements. Spectrophotometric, spectroscopic, and electrochemical determinations were performed under anaerobic conditions (except for **1**·2DMF) by using the equipment and procedures described elsewhere.[3] In cyclic voltammetry, the working electrode was a Pt disk, and an SCE reference electrode and 0.1 M $(Bu_4N)(ClO_4)$ supporting electrolyte were employed.

Results and Discussion

Preparation of $[Mn_2(salmp)_2]^{0,-,2-}$. Entry to the set of manganese complexes is readily afforded by Tsumaki's preparation[7] of the compound shown to be $Mn_2(salmp)_2$. Whereas $Fe_2(salmp)_2$ is most conveniently prepared by reaction of Fe^{III} with the preformed ligand,[3] the reaction of Mn^{II}, salicylaldehyde, and aqueous ammonia involves probable template formation of the ligand and the formation of an initial insoluble yellow solid, which is presumably $(NH_4)_2[Mn_2(salmp)_2]$. Suspension of this solid in boiling chloroform in the air resulted in the formation of a brown solution, from which black crystalline $Mn_2(salmp)_2$ was isolated and subsequently obtained in 52% purified yield as the bis(dimethylformamide) solvate. This compound is practically insoluble in common polar solvents; a more soluble derivative, $Mn_2(3\text{-}EtOsalmp)_2$, was prepared similarly.

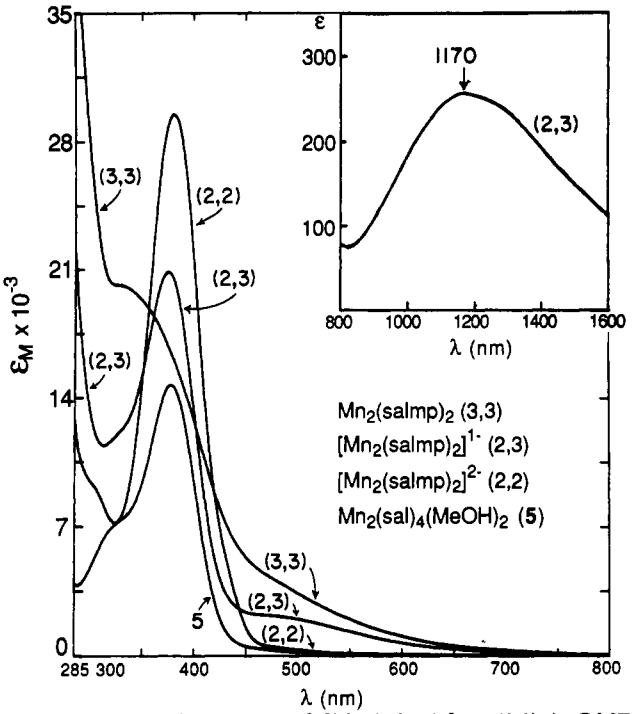

Figure 1. Absorption spectra of $[Mn_2(salmp)_2]$ = (3,3) in DMF, $[Mn_2(salmp)_2]^-$ = (2,3) and $[Mn_2(salmp)_2]^{2-}$ = (2,2) in acetonitrile, and $Mn_2(sal)_4(MeOH)_2$ (**5**) in methanol. Inset: near-IR region of the spectrum of (2,3) showing the intervalence band.

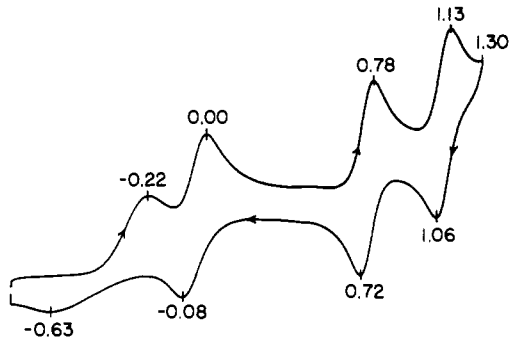

Figure 2. Cyclic voltammogram of $[Mn_2(salmp)_2]^{2-}$ in acetonitrile at 50 mV/s. Peak potentials vs SCE are indicated.

$Mn_2(salmp)_2$ is readily reduced. Thus, reaction 1 affords the mixed-valence $Mn^{III}Mn^{II}$ state as brown-black $[Mn_2(salmp)_2]^-$,

$$Mn_2(salmp)_2 + EtS^- \rightarrow [Mn_2(salmp)_2]^- + \tfrac{1}{2}EtSSEt \quad (1)$$

$$[Mn_2(salmp)_2]^- + EtS^- \rightarrow [Mn_2(salmp)_2]^{2-} + \tfrac{1}{2}EtSSEt \quad (2)$$

$$2Mn^{2+} + 4Hsal + 4Et_3N \rightarrow Mn_2(sal)_4(MeOH)_2 + 4Et_3NH^+ \quad (3)$$

isolated as its Et_4N^+ or Ph_4P^+ salt in 72–76% purified yield. A further reaction 2 results in reduction to the $Mn^{II}Mn^{II}$ state, which was obtained as orange $[Mn_2(salmp)_2]^{2-}$ in 42% purified yield as its Et_4N^+ salt. When the direct synthesis of this compound from Mn^{II} and salmp in methanol, as in the successful preparation of $[Fe_2(salmp)_2]^{2-}$,[3] was attempted, a sparingly soluble yellow solid was isolated. It was further ascertained that $[Mn_2(salmp)_2]^{2-}$ is prone to hydrolysis in the presence of small amounts of water and generates the same yellow solid. Thereafter, reaction 3 (Hsal = salicylaldehyde) in methanol was found to give this yellow compound (71%), in crystalline form, whose identity was established by X-ray diffraction.

The three compounds exhibit the absorption spectra set out in Figure 1. Like the spectra of their iron counterparts, these are dominated by $RO^- \rightarrow Mn$ CT bands near 380 nm. The most interesting feature is the broad near-IR band at λ_{max} (ϵ_M) = 1170

(17) See the paragraph at the end of this article concerning supplementary material available.
(18) Weigel, J. A.; Srivastava, K. K. P.; Day, E. P.; Münck, E.; Holm, R. H. *J. Am. Chem. Soc.* **1990**, *112*, 8015.
(19) Day, E. P.; Kent, T. A.; Lindahl, P. A.; Münck, E.; Orme-Johnson, W. H.; Roder, H.; Roy, A. *Biophys. J.* **1987**, *52*, 837.

Table III. Positional Parameters (×10⁴) for $(Ph_4P)[Mn_2(salmp)_2]\cdot 3.5DMF$ (3·3.5DMF)

atom	x/a	y/b	z/c
Mn(1)	2415 (1)	4164 (1)	3123 (1)
Mn(1′)	609 (1)	2954 (1)	2276 (1)
O(1)	2438 (3)	5243 (3)	3767 (2)
O(2)	3890 (3)	4270 (3)	3117 (2)
O(3)	2325 (3)	3220 (3)	2326 (2)
O(1′)	486 (3)	1777 (3)	1590 (2)
O(2′)	−967 (3)	3206 (3)	2256 (2)
O(3′)	926 (3)	3944 (3)	3209 (2)
N(1)	2023 (4)	5210 (3)	2321 (2)
N(2)	2574 (4)	2804 (3)	3660 (2)
N(1′)	1214 (4)	1845 (3)	3024 (2)
N(2′)	660 (4)	4302 (3)	1667 (2)
C(1)	2230 (5)	6121 (4)	2420 (3)
C(2)	3469 (5)	2440 (4)	3823 (3)
C(3)	1660 (5)	4839 (4)	1627 (3)
C(11)	2628 (5)	6611 (4)	3062 (3)
C(12)	2720 (5)	6158 (4)	3686 (3)
C(13)	3062 (5)	6738 (5)	4266 (3)
C(14)	3318 (6)	7711 (5)	4222 (4)
C(15)	3248 (6)	8150 (5)	3610 (4)
C(16)	2909 (5)	7597 (5)	3039 (3)
C(21)	4473 (5)	2883 (5)	3741 (3)
C(22)	4642 (5)	3720 (5)	3375 (3)
C(23)	5680 (5)	4004 (5)	3287 (3)
C(24)	6524 (6)	3506 (6)	3569 (3)
C(25)	6363 (6)	2716 (5)	3951 (3)
C(26)	5355 (5)	2396 (5)	4018 (3)
C(31)	2492 (5)	4207 (4)	1384 (3)
C(32)	2800 (5)	3415 (4)	1766 (3)
C(33)	3584 (5)	2831 (5)	1546 (3)
C(34)	4048 (5)	3020 (5)	970 (3)
C(35)	3765 (6)	3801 (5)	601 (3)
C(36)	2982 (5)	4401 (5)	801 (3)
C(1′)	1335 (5)	954 (4)	2873 (3)
C(2′)	−144 (5)	4626 (4)	1338 (3)
C(3′)	1628 (5)	2185 (4)	3716 (3)
C(11′)	1052 (5)	423 (4)	2221 (3)
C(12′)	669 (5)	863 (4)	1624 (3)
C(13′)	459 (5)	230 (5)	1036 (3)
C(14′)	603 (5)	−753 (5)	1042 (3)
C(15′)	970 (6)	−1172 (5)	1632 (4)
C(16′)	1198 (5)	−595 (5)	2212 (4)
C(21′)	−1229 (5)	4320 (4)	1358 (3)
C(22′)	−1577 (5)	3663 (4)	1841 (3)
C(23′)	−2675 (5)	3562 (5)	1867 (3)
C(24′)	−3375 (6)	4037 (6)	1446 (4)
C(25′)	−3021 (6)	4640 (5)	956 (4)
C(26′)	−1973 (5)	4775 (5)	926 (3)
C(31′)	825 (5)	2771 (4)	4044 (3)
C(32′)	516 (5)	3643 (4)	3776 (3)
C(33′)	−218 (5)	4179 (5)	4086 (3)
C(34′)	−679 (6)	3836 (5)	4648 (3)
C(35′)	−415 (6)	2967 (5)	4893 (3)
C(36′)	349 (6)	2431 (5)	4599 (3)

nm (270) in the spectrum of $[Mn_2(salmp)_2]^-$. This is assigned as an intervalence band, indicating that the monoanion is a type II mixed-valence species in the Robin–Day classification.[20] This band has been reported for only one other $Mn^{III}Mn^{II}$ complex.[21]

Electron-Transfer Series. The cyclic voltammogram of $[Mn_2(salmp)_2]^{2-}$ in acetonitrile, shown in Figure 2, reveals the existence of five oxidation levels in the $[Mn_2(salmp)_2]^z$ electron-transfer series (4). The 2−/1− potential is approximate

$$[Mn_2(salmp)_2]^{2-} \underset{}{\overset{-0.4\ V}{\rightleftharpoons}} [Mn_2(salmp)_2]^{-} \overset{-0.04\ V}{\rightleftharpoons}$$
$$Mn^{II}Mn^{II} \qquad Mn^{III}Mn^{II}$$
$$[Mn_2(salmp)_2]^{0} \overset{+0.75\ V}{\rightleftharpoons} [Mn_2(salmp)_2]^{+} \overset{+1.10\ V}{\rightleftharpoons}$$
$$Mn^{III}Mn^{III} \qquad Mn^{IV}Mn^{III}$$
$$[Mn_2(salmp)_2]^{2+} \quad (4)$$
$$Mn^{IV}Mn^{IV}$$

(20) Robin, M. D.; Day, P. *Adv. Inorg. Chem. Radiochem.* **1967**, *10*, 247.
(21) Okawa, H.; Honda, A.; Nakamura, M.; Kida, S. *J. Chem. Soc., Dalton Trans.* **1985**, 59.

Table IV. Positional Parameters (×10⁴) for $(Et_4N)_2[Mn_2(salmp)_2]\cdot 4CH_3CN$ (4·4CH_3CN)

atom	x/a	y/b	z/c
Mn(1)	5493.0 (7)	862.1 (4)	162.9 (4)
O(1)	7137 (4)	1465 (3)	181 (2)
O(2)	4787 (4)	1903 (2)	476 (2)
O(3)	4166 (3)	107 (2)	546 (2)
N(1)	6807 (3)	248 (2)	1231 (2)
N(2)	3903 (4)	1043 (2)	−979 (2)
C(1)	7949 (4)	415 (3)	1542 (3)
C(2)	3150 (5)	1600 (3)	−1104 (3)
C(3)	3638 (4)	432 (3)	−1587 (3)
C(11)	8652 (4)	1035 (3)	1321 (3)
C(12)	8202 (5)	1530 (3)	668 (3)
C(13)	9027 (6)	2116 (4)	563 (4)
C(14)	10183 (6)	2198 (4)	1047 (4)
C(15)	10602 (6)	1706 (4)	1682 (4)
C(16)	9850 (5)	1139 (4)	1807 (4)
C(21)	3135 (5)	2272 (3)	−624 (3)
C(22)	3963 (5)	2392 (3)	133 (3)
C(23)	3834 (7)	3096 (4)	508 (4)
C(24)	2959 (7)	3626 (4)	175 (5)
C(25)	2147 (7)	3497 (4)	−548 (5)
C(26)	2241 (6)	2825 (4)	−938 (4)
C(31)	4748 (5)	234 (3)	−1868 (3)
C(32)	5819 (4)	−33 (3)	−1313 (3)
C(33)	6841 (5)	−216 (4)	−1602 (4)
C(34)	6791 (7)	−151 (4)	−2403 (4)
C(35)	5746 (7)	103 (4)	−2940 (4)
C(36)	4719 (6)	292 (3)	−2670 (3)

Table V. Positional Parameters (×10⁴) for $[Mn_2(sal)_4(MeOH)_2]\cdot MeOH$ (5·MeOH)

atom	x/a	y/b	z/c
Mn(1)	8153 (1)	9156.8 (7)	1832 (1)
Mn(2)	6445 (1)	8482.0 (7)	3148 (1)
O(1)	6677 (5)	8783 (3)	600 (5)
O(2)	7412 (7)	8667 (4)	4713 (5)
O(3)	7760 (7)	10164 (4)	1219 (6)
O(4)	6974 (6)	9448 (3)	2737 (5)
O(5)	9173 (6)	9064 (4)	708 (5)
O(6)	9735 (5)	9435 (4)	2805 (5)
O(7)	6439 (7)	7451 (4)	3554 (6)
O(8)	7955 (5)	8242 (3)	2618 (5)
O(9)	4813 (8)	8622 (4)	3543 (7)
O(10)	5388 (6)	8270 (4)	1692 (5)
C(1)	5892 (11)	9202 (7)	−83 (10)
C(2)	7430 (13)	8265 (7)	5592 (9)
C(10)	7294 (10)	10609 (5)	1565 (9)
C(11)	6729 (8)	10603 (5)	2394 (8)
C(12)	6639 (8)	10031 (5)	2973 (7)
C(13)	6136 (9)	10111 (6)	3809 (8)
C(14)	5739 (11)	10713 (6)	4045 (10)
C(15)	5802 (13)	11275 (6)	3450 (12)
C(16)	6331 (12)	11219 (5)	2656 (11)
C(20)	10158 (9)	9292 (5)	761 (7)
C(21)	10958 (8)	9571 (5)	1631 (7)
C(22)	10687 (8)	9636 (5)	2613 (7)
C(23)	11593 (10)	9898 (6)	3408 (7)
C(24)	12622 (9)	10093 (6)	3223 (8)
C(25)	12879 (9)	10028 (6)	2284 (8)
C(26)	12004 (9)	9784 (5)	1475 (8)
C(30)	7217 (11)	7041 (5)	3561 (8)
C(31)	8254 (8)	7123 (5)	3220 (7)
C(32)	8574 (8)	7708 (5)	2760 (7)
C(33)	9655 (9)	7670 (5)	2476 (8)
C(34)	10317 (10)	7119 (6)	2602 (9)
C(35)	9977 (10)	6556 (6)	3042 (9)
C(36)	8988 (10)	6562 (5)	3353 (8)
C(40)	3852 (12)	8469 (6)	3030 (13)
C(41)	3484 (10)	8219 (6)	2019 (11)
C(42)	4303 (9)	8132 (5)	1375 (9)
C(43)	3828 (11)	7896 (6)	379 (10)
C(44)	2662 (14)	7755 (7)	16 (13)
C(45)	1916 (13)	7844 (8)	631 (19)
C(46)	2330 (11)	8079 (7)	1590 (16)
C(3)	530 (17)	6042 (9)	363 (14)
O(11)	−551 (8)	5842 (4)	−289 (7)

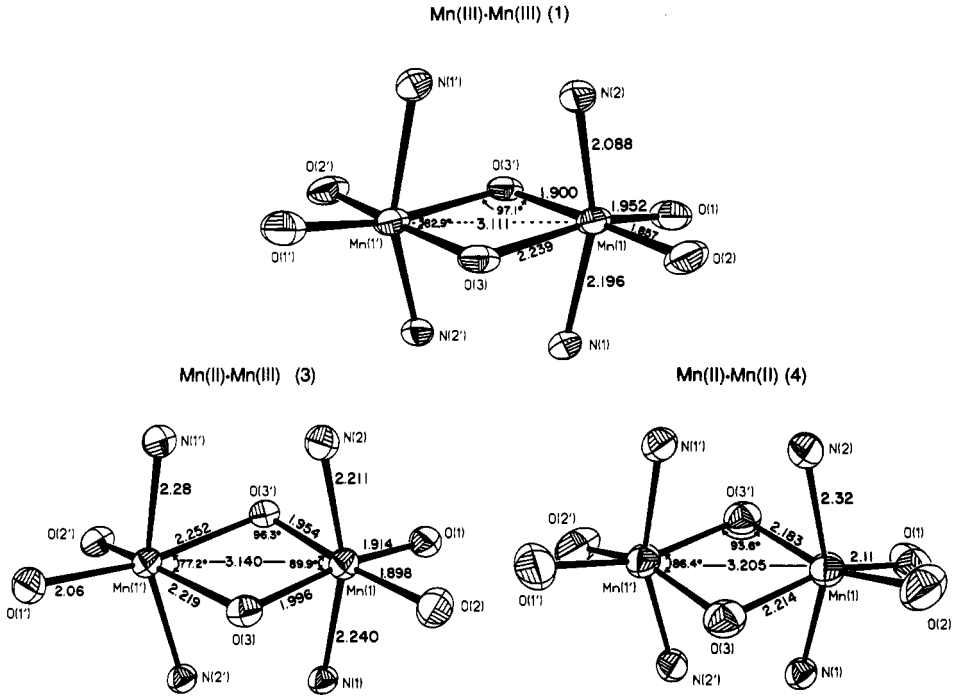

Figure 3. Structures of the coordination units of $Mn_2(salmp)_2$ (1·2MeCN), $[Mn_2(salmp)_2]^-$ (3·3.5DMF), and $[Mn_2(salmp)_2]^{2-}$ (4·4MeCN), showing 50% probability ellipsoids and the atom-labeling schemes. In the $Mn^{III}Mn^{III}$ and $Mn^{II}Mn^{II}$ units, the primed and unprimed atoms are related by a center of symmetry; bond distances at Mn(1') in **3** and Mn(1) in **4** are average values.

because this step is not electrochemically reversible, presumably because of the structural rearrangement involved (vide infra). It is, however, chemically reversible. When it was examined separately at a slow scan rate (10 mV/s), ΔE_p was reduced to 330 mV and $i_{pc}/i_{pa} \approx 1$. Coulometric oxidation and reduction of this step showed it to be a one-electron process. The remaining steps are essentially reversible ($i_{pc}/i_{pa} \approx 1$, ΔE_p = 60–80 mV) and correspond to one-electron reactions. Coulometry of succeeding reactions in the series,[22] as well as attempts to prepare pure samples of the 1+ and 2+ complexes, was hampered by the insolubility of $Mn_2(salmp)_2$.

Among related binuclear complexes, the first two steps in series (4) have been previously observed in species with one and two phenolate bridges.[23a-d,24d] These species are cationic or neutral in the $Mn^{II}Mn^{II}$ state; their oxidations to the $Mn^{III}Mn^{II}$ and $Mn^{III}Mn^{III}$ states occur at or above ca. +0.4 and +1.0 V vs SCE, respectively. In contrast, the dianionic nature of the $Mn^{II}Mn^{II}$ complex in series (4) would appear to contribute to a significant lowering of the potentials (ca. −0.4, −0.04 V) required to reach these states. The effect of charge places the last two oxidations, represented as metal-centered reactions, within observable range. In all other cases of $Mn^{IV}Mn^{III}$ and $Mn^{IV}Mn^{IV}$ complexes, the bridges consist of two[25,26d] or three[26d] μ-oxo, two μ-oxo and one μ-RCO_2,[24e] or one μ-oxo and two μ-RCO_2[26] groups. These species are cations, frequently with neutral terminal ligands, and the $Mn^{IV}Mn^{III}$ and $Mn^{IV}Mn^{IV}$ states are usually achieved at potentials in excess of about +0.3 and +1.2 V vs SCE, respectively. The polarizable, electron-rich oxide bridges certainly promote the stabilities of these highly oxidized forms. While we have not proven that the 1+ and 2+ species in series (4) contain the indicated Mn oxidation states because of our inability thus far to isolate them,[27] it appears plausible that charge effects could reduce the otherwise far more positive potentials expected for generation of the $[Mn_2(OPh)_2]^{5+,6+}$ bridge units to the observed values. In any event, series (4) is one of the most extensive electron-transfer arrays for binuclear manganese. It is the only example in which the three lower oxidation levels have been isolated with the *same* bridging and terminal ligands.

Structures of $[Mn_2(salmp)_2]^{0,-,2-}$. As pointed out earlier,[3] the salmp ligand cannot act as a mononuclear pentadentate ligand. It is, however, dimensionally correct to form bridged binuclear complexes with metal ions whose octahedral high-spin radii span

(22) The electrochemistry of the more soluble compound Mn_2(3-EtOsalmp)$_2$ was not well-behaved.

(23) $[Mn_2(\mu\text{-OPh})(\mu\text{-}O_2R)_2]$ bridges: (a) Suzuki, M.; Mikuriya, M.; Murata, S.; Uehara, A.; Oshio, H.; Kida, S.; Saito, K. *Bull. Chem. Soc. Jpn.* **1987**, *60*, 4305. (b) Suzuki, M.; Murata, S.; Uehara, A.; Kida, S. *Chem. Lett.* **1987**, 281. (c) Buchanan, R. M.; Oberhausen, K. J.; Richardson, J. F. *Inorg. Chem.* **1988**, *27*, 973. (d) Diril, H.; Chang, H.-R.; Nilges, M. J.; Zhang, X.; Potenza, J. A.; Schugar, H. J.; Isied, S. S.; Hendrickson, D. N. *J. Am. Chem. Soc.* **1989**, *111*, 5102. (e) Mikuriya, M.; Fujii, T.; Kamisawa, S.; Kawasaki, Y.; Tokii, T.; Oshio, H. *Chem. Lett.* **1990**, 1184.

(24) $[Mn_2(\mu\text{-OPh})_2]$ and $[Mn_2(\mu\text{-OPh})_2(\mu\text{-X})]$ bridges: (a) Vincent, J. B.; Folting, K.; Huffman, J. C.; Christou, G. *Inorg. Chem.* **1986**, *25*, 996. (b) Nishida, Y. *Chem. Lett.* **1987**, 2151. (c) Coucouvanis, D.; Greiwe, K.; Salifoglou, A.; Challen, P.; Simopoulos, A.; Kostikas, A. *Inorg. Chem.* **1988**, *27*, 594. (d) Chang, H.-R.; Larsen, S. K.; Boyd, P. D. W.; Pierpont, C. G.; Hendrickson, D. N. *J. Am. Chem. Soc.* **1988**, *110*, 4565. (e) Bashkin, J. S.; Schake, A. R.; Vincent, J. B.; Chang, H.-R.; Li, Q.; Huffman, J. C.; Christou, G.; Hendrickson, D. N. *J. Chem. Soc., Chem. Commun.* **1988**, 700. (f) Hodgson, D. J.; Schwartz, B. J.; Sorrell, T. N. *Inorg. Chem.* **1989**, *28*, 2226.

(25) $[Mn_2(\mu\text{-}O)_2]$ bridges: (a) Suzuki, M.; Senda, H.; Kobayashi, Y.; Oshio, H.; Uehara, A. *Chem. Lett.* **1988**, 1763. (b) Hagen, K. S.; Armstrong, W. H.; Hope, H. *Inorg. Chem.* **1988**, *27*, 969. (c) Brewer, K. J.; Calvin, M.; Lumpkin, R. S.; Otvos, J. W.; Spreer, L. O. *Inorg. Chem.* **1989**, *28*, 4446. (d) Oki, A. R.; Glerup, J.; Hodgson, D. J. *Inorg. Chem.* **1990**, *29*, 2435. (e) Bossek, U.; Weyhermüller, T.; Wieghardt, K.; Nuber, B.; Weiss, J. *J. Am. Chem. Soc.* **1990**, *112*, 6387. This reference describes a complex with the $[Mn_2(\mu\text{-}O)_2(\mu\text{-}O_2)]$ bridge.

(26) $[Mn_2(\mu\text{-}O)(\mu\text{-}RCO_2)_2]$ bridges: (a) Wieghardt, K.; Bossek, U.; Bonvoisin, J.; Beauvillain, P.; Girerd, J.-J.; Nuber, B.; Weiss, J.; Heinze, J. *Angew. Chem., Int. Ed. Engl.* **1986**, *25*, 1030. (b) Sheats, J. E.; Czernuszewicz, R. S.; Dismukes, G. C.; Rheingold, A. L.; Petrouleas, V.; Stubbe, J.; Armstrong, W. H.; Beer, R. H.; Lippard, S. J. *J. Am. Chem. Soc.* **1987**, *109*, 1435. (c) Ménage, S.; Girerd, J.-J.; Gleizes, A. *J. Chem. Soc., Chem. Commun.* **1988**, 431. (d) Wieghardt, K.; Bossek, U.; Nuber, B.; Weiss, J.; Bonvoisin, J.; Corbella, M.; Vitols, S. E.; Girerd, J.-J. *J. Am. Chem. Soc.* **1988**, *110*, 7398. (e) Bossek, U.; Wieghardt, K.; Nuber, B.; Weiss, J. *Inorg. Chim. Acta* **1989**, *165*, 123. (f) Wu, F.-J.; Kurtz, D. M., Jr.; Hagen, K. S.; Nyman, P. D.; Debrunner, P. G.; Vankai, V. A. *Inorg. Chem.* **1990**, *29*, 5174. The citations here and in ref 23 are illustrative of the indicated structural types but not exhaustive; additional references are available elsewhere.[9-15]

(27) Ligand-based oxidation of manganese(II) salicylaldiminato complexes (but without direct detection of the radical species) has been claimed: Matsushita, T.; Spencer, L.; Sawyer, D. T. *Inorg. Chem.* **1988**, *27*, 1167.

the (minimal) range 0.78 Å (Fe^{3+}, Mn^{3+}) to 0.97 Å (Mn^{2+}).[28] The trans-C_{2h} conformation of the complexes, illustrated schematically as

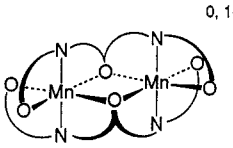

1 - 4

is invariant with oxidation state. Each metal atom is coordinated in a distorted octahedral arrangement with the two octahedra sharing a common edge defined by the bridging phenolate oxygen atoms. The stability of the manganese and iron complexes derives in considerable part from the fact that each salmp ligand supplies both bridging and terminal binding sites. The susceptibility of $[Mn_2(salmp)_2]^{2-}$ toward hydrolysis suggests that a stability limit may be approached or exceeded by the coordination of two divalent ions with radii of ca. 1.0 Å. Selected interatomic distances and angles are contained in Table VI. The structures of $[Mn_2(salmp)_2]^{0,2-}$ have crystallographically imposed centrosymmetry; no symmetry is imposed on $[Mn_2(salmp)_2]^-$. Because of the structural similarities to the series $[Fe_2(salmp)_2]^{0,-,2-}$, whose structures have been described in detail,[3] only the leading structural features in the manganese series are described.

Of principal interest are the comparative structural details over the three oxidation levels. The structures of the coordination units are provided in Figure 3. Each has a planar $Mn_2(\mu\text{-}O)_2$ bridge unit, which is a rhombus in $[Mn_2(salmp)_2]^{2-,0}$ but is an irregular quadrilateral in $[Mn_2(salmp)_2]^-$. Terminal bond distances and the Mn···Mn separations tend to decrease with increasing oxidation level, consistent with the smaller size of Mn^{III}. Starting with $[Mn_2(salmp)_2]^{2-}$, it is evident from angular distortions from idealized octahedral coordination that the molecule is strained. Thus, the dihedral angles O(1,2)Mn(1)O(3,3′) = 28.3° and O(1,2)Mn(1)N(1,2) = 65.7° instead of 0 and 90°, respectively. In $Mn_2(salmp)_2$, these angles are 13.5 and 83.8°, suggesting a better fit in the binuclear structure with Mn^{III}. Among binuclear doubly bridged Mn^{II} complexes,[23e,24b,c,f,29] the Mn–O–Mn bridge angle of 93.6 (1)° is the smallest, and the Mn···Mn distance of 3.205 (1) Å is one of the shortest,[24c,29b] yet reported.

A number of features are nearly constant across the series. In particular, the bridge angles Mn(1)–O(3,3′)–Mn(1′) change from 93.6 (1) to 97.1 (1)° and the larger angular distortions from idealized octahedral geometry at the metal sites remain nearly invariant. These include O(1)–Mn(1)–O(3) (160.4 (1)–166.0 (1)°), N(1)–Mn(1)–N(2) (156.8 (1)–159.1 (1)°), O(3)–Mn(1)–N(1) (79.8 (1)–82.0 (2)°), and O(1)–Mn(1)–N(2) (109.6 (2)–114.8 (1)°). From their small range of values, we conclude that, as in the iron series,[3] they are set by the binucleating ligand structure. The bridge dihedral angle Mn_2N_4/Mn_2O_2 is also nearly constant but with more regular values (88.4–93.9°).

The most conspicuous structural feature of $Mn_2(salmp)_2$ is the Jahn–Teller distortion, which results in a very large difference (0.34 Å) in bridging Mn–O distances and an otherwise pseudoaxial elongation.[30] This type of axial distortion is usual in mononuclear Mn^{III} complexes, but there is at least one case of axial compression in a binuclear complex.[31] The Mn···Mn distance of 3.111 (1) Å is shorter than that in the only other structurally characterized $Mn^{III}_2(\mu\text{-}OPh)_2$ complex, $[Mn_2(slt)_4(py)_2]^{2-}$ (3.247 Å; slt = salicylate),[24a] but is longer than those in two bis(μ-alkoxo)-bridged species (2.869, 2.931 Å).[32] The structures of $[Mn_2(salmp)_2]^{0,2-}$ allow identification of $[Mn_2(salmp)_2]^-$ as a trapped-valence complex. The longer bond distances and less pronounced distortion show the Mn(1′) site to contain Mn^{II}. Similarly, at the Mn(1) = Mn^{III} site, bond distances are shorter and a low-symmetry distortion is more evident. On a similar basis, the five other structurally characterized $Mn^{III}Mn^{II}$ complexes are also trapped-valence.[23a,c,d,24d,e] In $[Mn_2(salmp)_2]^-$, the two sites are tightly coupled inasmuch as neither of their structures is only a slightly modified version of those in the $Mn^{II}Mn^{II}$ and $Mn^{III}Mn^{III}$ complexes. We note also that $[Fe_2(salmp)_2]^-$ is trapped-valence in crystals of $(Et_4N)[Fe_2(salmp)_2]$.[3] Here there is no Jahn–Teller

Table VI. Selected Interatomic Distances (Å) and Angles (deg) for $Mn_2(salmp)_2\cdot 2CH_3CN$ (**1**·2CH_3CN), $(Ph_4P)[Mn_2(salmp)_2]\cdot 3.5DMF$ (**3**·3.5DMF), and $(Et_4N)_2[Mn_2(salmp)_2]\cdot 4CH_3CN$ (**4**·4CH_3CN)

	1·2CH_3CN[a]	**3**·3.5DMF	**4**·4CH_3CN[a]
Mn(1)···Mn(1′)	3.111 (1)	3.140 (1)	3.205 (1)
O(3)···O(3′)	2.753 (5)	2.791 (8)	3.010 (7)
Mn(1)–O(3)	2.239 (3)	1.996 (4)	2.214 (3)
Mn(1)–O(3′)	1.900 (3)	1.954 (4)	2.183 (3)
Mn(1′)–O(3)		2.219 (4)	
Mn(1′)–O(3′)		2.252 (4)	
Mn(1)–O(1)	1.952 (3)	1.914 (4)	2.117 (4)
Mn(1)–O(2)	1.857 (3)	1.898 (4)	2.107 (4)
Mn(1)–N(1)	2.196 (3)	2.240 (5)	2.316 (4)
Mn(1)–N(2)	2.088 (3)	2.211 (5)	2.324 (4)
Mn(1′)–O(1′)		2.064 (4)	
Mn(1′)–O(2′)		2.061 (4)	
Mn(1′)–N(1′)		2.294 (5)	
Mn(1′)–N(2′)		2.272 (5)	
Mn(1)–O(3)–Mn(1′)	97.1 (1)	96.2 (2)	93.6 (1)
Mn(1)–O(3′)–Mn(1′)		96.4 (2)	
O(3)–Mn(1)–O(3′)	82.9 (1)	89.9 (2)	86.4 (1)
O(3)–Mn(1′)–O(3′)		77.2 (1)	
O(3)–Mn(1)–O(1)	166.0 (1)	169.4 (2)	160.4 (1)
O(3)–Mn(1)–O(2)	91.0 (1)	90.8 (2)	96.2 (2)
O(3′)–Mn(1)–O(1)	93.0 (1)	89.9 (2)	96.6 (2)
O(3′)–Mn(1)–O(2)	173.6 (1)	173.3 (2)	160.9 (1)
O(3)–Mn(1′)–O(1′)		98.6 (2)	
O(3)–Mn(1′)–O(2′)		160.8 (2)	
O(3′)–Mn(1′)–O(1′)		164.6 (2)	
O(3′)–Mn(1′)–O(2′)		90.7 (2)	
O(3)–Mn(1)–N(1)	79.9 (1)	82.0 (2)	79.8 (1)
O(3)–Mn(1)–N(2)	80.1 (1)	81.0 (2)	84.8 (1)
O(3′)–Mn(1)–N(1)	85.2 (1)	89.5 (2)	85.8 (1)
O(3′)–Mn(1)–N(2)	86.4 (1)	83.8 (2)	80.3 (1)
O(3)–Mn(1′)–N(1′)		77.7 (2)	
O(3)–Mn(1′)–N(2′)		80.5 (2)	
O(3′)–Mn(1′)–N(1′)		80.6 (2)	
O(3′)–Mn(1′)–N(2′)		87.3 (2)	
O(1)–Mn(1)–O(2)	93.3 (2)	90.6 (2)	87.2 (2)
O(1)–Mn(1)–N(1)	86.5 (1)	87.3 (2)	81.1 (1)
O(2)–Mn(1)–N(1)	95.4 (1)	97.1 (2)	113.3 (1)
O(1)–Mn(1)–N(2)	113.2 (1)	109.6 (2)	114.8 (1)
O(2)–Mn(1)–N(2)	90.9 (1)	89.8 (2)	81.2 (1)
N(1)–Mn(1)–N(2)	159.1 (1)	161.7 (2)	159.8 (1)
O(1′)–Mn(1′)–O(2′)		96.8 (2)	
O(1′)–Mn(1′)–N(1′)		84.0 (2)	
O(2′)–Mn(1′)–N(1′)		115.4 (2)	
O(1′)–Mn(1′)–N(2′)		106.8 (2)	
O(2′)–Mn(1′)–N(2′)		84.1 (2)	
N(1′)–Mn(1′)–N(2′)		156.9 (2)	

[a] Primed and unprimed atoms related by a crystallographically imposed inversion center.

(28) Shannon, R. D. *Acta Crystallogr.* **1976**, *A32*, 751.
(29) (a) Kessissoglou, D. P.; Butler, W. M.; Pecoraro, V. L. *Inorg. Chem.* **1987**, *26*, 495. (b) Jones, R. A.; Koschmieder, S. U.; Nunn, C. M. *Inorg. Chem.* **1988**, *27*, 4526. (c) Carducci, M. D.; Doedens, R. J. *Inorg. Chem.* **1989**, *28*, 2492.
(30) The structure of Mn_2(3-OEtsalmp)$_2$·EtCN was determined to see if a substituent placed so as potentially to interact with the N–C–N portion of the bridge structure would affect the nature of the distortions around Mn^{III}. This compound crystallizes in triclinic space group $P\bar{1}$ with a = 10.488 (1) Å, b = 11.167 (2) Å, c = 12.149 (2) Å, α = 107.49 (1)°, β = 99.40 (1)°, γ = 90.13 (1)°, and Z = 1. The structure was refined to R (R_w) = 7.8% (10.8%). The molecular conformation and distortions are the same as, and bond distances and angles differ trivially from, those of $Mn_2(salmp)_2$. Full details are available elsewhere: Yu, S. Ph.D. Thesis, Harvard University, 1991.
(31) Saadeh, S. M.; Lah, M. S.; Pecoraro, V. L. *Inorg. Chem.* **1991**, *30*, 8.
(32) (a) Mikuriya, M.; Torihara, N.; Okawa, H.; Kida, S. *Bull. Chem. Soc. Jpn.* **1981**, *54*, 1063. (b) Nishida, Y.; Oshino, N.; Tokii, T. *Z. Naturforsch.* **1988**, *43B*, 472.

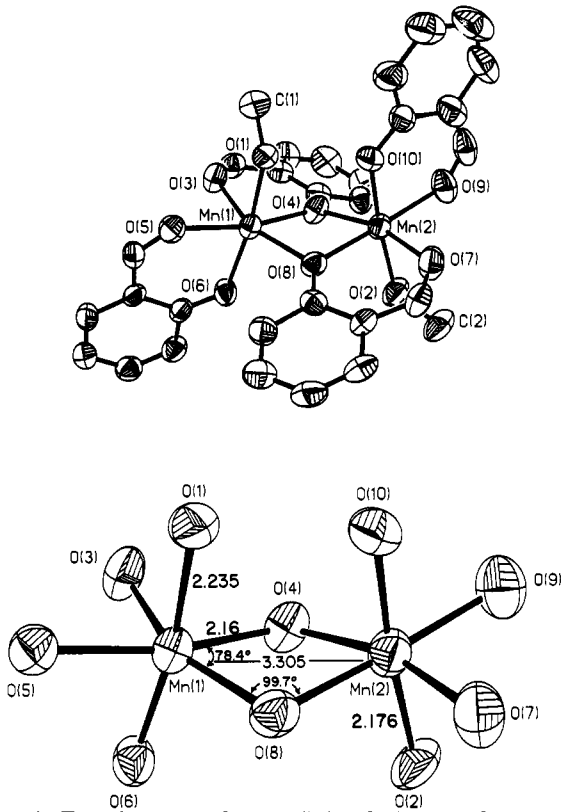

Figure 4. Top: Structure of $Mn_2(sal)_4(MeOH)_2$ (**5**·MeOH), showing 40% probability ellipsoids and the atom-labeling scheme. Bottom: Coordination unit (50% ellipsoids) with selected bond distances and angles.

effect to differentiate sites,[33] which must be accomplished by metal ion size differences. Evidently, the binucleating conformation of the salmp ligand is sufficiently rigid to transmit structural differences at one site to the other when there is passage from a homovalent to a mixed-valent species.

Structure of $Mn_2(sal)_4(MeOH)_2$. Previous studies of manganese(II) salicylaldehyde complexes were restricted to determination of formation constants of a compound formulated as $Mn(sal)_2$.[34] While a solvated mononuclear species may exist in solution, the isolated product of reaction 4 has the binuclear, roughly centrosymmetric structure shown in Figure 4 with the metric parameters in Table VII. The molecule is built up with one salicylaldehyde anion as a terminal ligand at each Mn atom, one methanol molecule trans to the phenolate oxygen atom at each metal site, and two salicylaldehyde anions functioning each as a bridging and terminal ligand. The bridges are phenolate oxygen atoms, and the $Mn^{II}_2O_2$ bridge unit is planar. The MnO_6 coordination units are distorted octahedra with the four types of Mn–O bond lengths (Å) in the order Mn–O_t(Ph) (2.10) < Mn–O_b (2.16 (1)) ≈ Mn–O_t(C=O) (2.17 (2)) < Mn–O_t(MeOH) (2.21) (t = terminal, b = bridging). The overall structure is similar to that of $[Mn_2(slt)_4(py)_2]^{2-}$, except that pyridine ligands are trans to the bridge phenolate oxygen atoms whereas the methanol ligands are cis. This structure establishes the nature of the final hydrolysis product of $[Mn_2(salmp)_2]^{2-}$. Given the strong bridge binding, it seems likely that the binuclear structure will be retained in methanol and other polar organic solvents.

Magnetism. We have established that the preparative compounds containing $[Mn_2(salmp)_2]^{0,-2}$ are all antiferromagnetically coupled, as opposed to the ferromagnetism of the corresponding iron series.[3,35] We report here the completed magnetic study of $Mn_2(salmp)_2$·2DMF. The spin Hamiltonian (5) (i = 1, 2) applies

$$H = \sum_i H_i + H_{ex} \tag{5}$$

$$H_i = D_i[(S_{zi}^2 - 2) + (E_i/D_i)(S_{xi}^2 - S_{yi}^2)] + \mu_B \mathbf{S}_i \cdot \mathbf{g}_i \cdot \mathbf{H} \tag{6}$$

$$H_{ex} = J\mathbf{S}_1 \cdot \mathbf{S}_2 \tag{7}$$

to the exchange-coupled binuclear Mn^{III} center. Antiferromagnetic exchange is described by a positive value of the coupling constant J; D_i and E_i are the zero-field splitting parameters of the two S_i = 2 Mn^{III} sites, and $\mathbf{g}_i$ are their **g** tensors. For present purposes, $g_{xi} = g_{yi} = g_{zi} = g_i$. The magnetic data, collected at 2–300 K at four fields between 0.2 and 5.5 T, are presented in two ways in Figure 5, where the solid lines are the best fit to the data with the parameter set (8). In Figure 5A, the striking feature is the

$$D_i = 3.1\ (7)\ \text{cm}^{-1} \qquad E_i/D_i = 0.22\ (5) \qquad g_i = 1.96\ (8)$$
$$J = 6.5\ (2)\ \text{cm}^{-1} \tag{8}$$

magnetic field dependence of the molar susceptibility. The susceptibility at the highest field is largest at the lower temperatures (relative to those at other fields at these temperatures). This effect arises from field-induced uncoupling of the antiferromagnetically coupled spins. The maximum in the data at 20 K arises from the interplay of two factors. The zero-field splitting and the saturation magnetization both favor the lowest field susceptibility being largest at low temperatures,[36] whereas the weak antiferromagnetic exchange coupling favors the highest field susceptibility being largest at low temperatures (due to field-induced decoupling). The same data and fit are plotted as μ_{eff}^2 vs temperature in Figure 5B,

Table VII. Selected Interatomic Distances (Å) and Angles (deg) for $Mn_2(sal)_4(MeOH)_2$·MeOH (**5**·MeOH)

Mn(1)–O(4)	2.155 (7)	Mn(2)–O(4)	2.171 (6)
Mn(1)–O(8)	2.179 (6)	Mn(2)–O(8)	2.146 (6)
Mn(1)–O(1)	2.235 (7)	Mn(2)–O(2)	2.176 (7)
Mn(1)–O(3)	2.210 (8)	Mn(2)–O(7)	2.163 (8)
Mn(1)–O(5)	2.169 (7)	Mn(2)–O(9)	2.153 (8)
Mn(1)–O(6)	2.092 (6)	Mn(2)–O(10)	2.102 (7)
O(1)–C(1)	1.42 (1)	O(2)–C(2)	1.44 (1)
O(3)–C(10)	1.21 (1)	O(7)–C(30)	1.24 (1)
O(4)–C(12)	1.31 (1)	O(8)–C(32)	1.30 (1)
O(5)–C(20)	1.25 (1)	O(9)–C(40)	1.22 (2)
O(6)–C(22)	1.29 (1)	O(10)–C(42)	1.29 (1)
O(4)–Mn(1)–O(8)	78.2 (2)	Mn(1)–O(4)–Mn(2)	99.6 (3)
O(4)–Mn(2)–O(8)	78.5 (3)	Mn(1)–O(8)–Mn(2)	99.7 (3)
O(1)–Mn(1)–O(3)	88.8 (3)	O(2)–Mn(2)–O(4)	88.5 (3)
O(1)–Mn(1)–O(4)	90.7 (3)	O(2)–Mn(2)–O(7)	87.4 (3)
O(1)–Mn(1)–O(5)	85.6 (2)	O(2)–Mn(2)–O(8)	94.3 (3)
O(1)–Mn(1)–O(8)	85.1 (3)	O(2)–Mn(2)–O(9)	91.8 (3)
O(3)–Mn(1)–O(4)	81.5 (3)	O(4)–Mn(2)–O(9)	106.2 (3)
O(3)–Mn(1)–O(5)	85.5 (3)	O(4)–Mn(2)–O(10)	95.2 (3)
O(3)–Mn(1)–O(6)	93.5 (3)	O(7)–Mn(2)–O(8)	85.4 (3)
O(4)–Mn(1)–O(6)	100.4 (3)	O(7)–Mn(2)–O(9)	90.4 (3)
O(5)–Mn(1)–O(6)	83.8 (3)	O(7)–Mn(2)–O(10)	90.0 (3)
O(5)–Mn(1)–O(8)	114.3 (3)	O(8)–Mn(2)–O(10)	90.0 (3)
O(6)–Mn(1)–O(8)	96.4 (3)	O(9)–Mn(2)–O(10)	83.6 (3)
O(4)–Mn(1)–O(5)	166.5 (3)	O(4)–Mn(2)–O(7)	163.1 (3)
O(1)–Mn(1)–O(6)	168.9 (2)	O(8)–Mn(2)–O(9)	172.4 (3)
O(3)–Mn(1)–O(8)	158.6 (3)	O(2)–Mn(2)–O(10)	174.8 (3)
Mn(1)–O(1)–C(1)	102.9 (6)	Mn(2)–O(2)–C(2)	126.9 (7)
Mn(1)–O(3)–C(10)	128.3 (7)	Mn(2)–O(4)–C(12)	128.9 (6)
Mn(1)–O(4)–C(12)	131.5 (6)	Mn(2)–O(7)–C(30)	127.0 (7)
Mn(1)–O(5)–C(20)	127.4 (6)	Mn(2)–O(8)–C(32)	129.1 (6)
Mn(1)–O(6)–C(22)	131.2 (6)	Mn(2)–O(9)–C(40)	126.9 (8)
Mn(1)–O(8)–C(32)	131.3 (6)	Mn(2)–O(10)–C(42)	132.6 (7)

(33) This does not imply that Jahn–Teller distortions necessarily produce structural differentiation sufficient for crystallographic detection. For an instructive example involving binuclear Mn and probable static disorder, cf.: Stebler, M.; Ludi, A.; Bürgi, H.-B. *Inorg. Chem.* **1986**, *25*, 4743.

(34) (a) Leussing, D. L.; Bai, K. S. *Anal. Chem.* **1968**, *40*, 575. (b) Kamat, P. V.; Laxmeshwar, N. B.; Datar, M. G. *J. Ind. Chem. Soc.* **1969**, *46*, 345.

(35) For recent related work, cf.: Fallon, G. D.; Markiewicz, A.; Murray, K. S.; Quach, T. *J. Chem. Soc., Chem. Commun.* **1991**, 198.

(36) For a related case, cf. Figure 3 in ref 18.

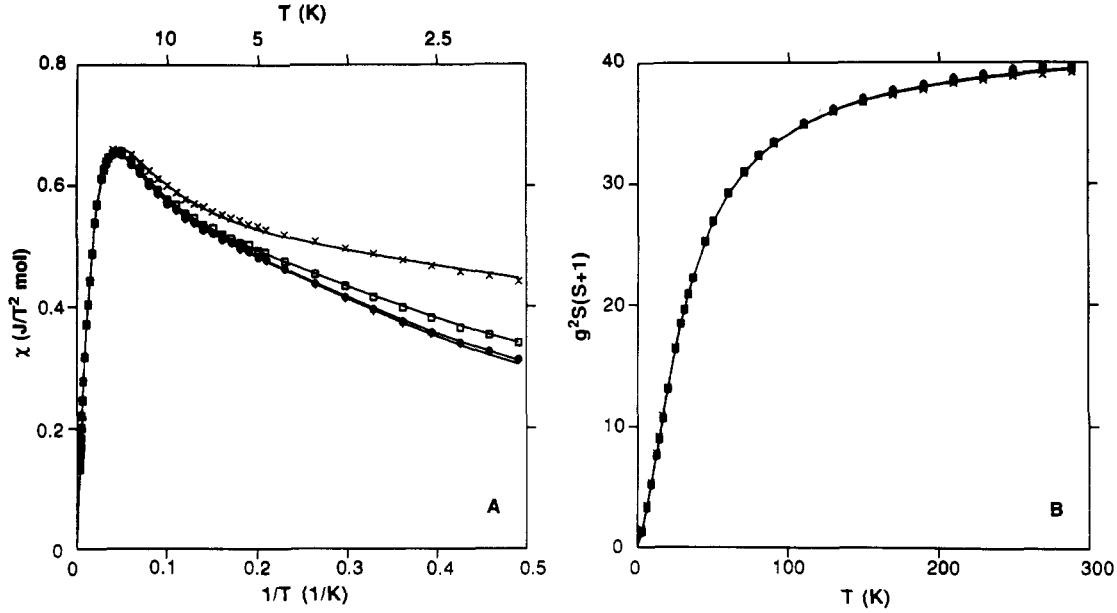

Figure 5. (A) Temperature dependence of the magnetic susceptibility of $Mn_2(salmp)_2 \cdot 2DMF$ over the range 2–300 K at fields of 0.20 (+), 1.375 (○), 2.75 (□), and 5.50 (×) T. The solid lines were calculated from the spin Hamiltonian (5) for identical exchange-coupled Mn^{III} sites with $S_i = 2$ and the parameter set (8). An iterative process described in the Experimental Section was used to show that 0.3% of the Mn^{III} was present as a mononuclear $S = 2$ impurity, which has been subtracted from the data. The amount of binuclear complex in the sample was 4.1 (1) μmol, and the amount measured by weight was 4.03 μmol. (B) Data and fit of (A) plotted as $\mu_{eff}^2 = g^2S(S+1)$ vs temperature. A majority of the points below 12 K have been omitted for clarity.

which highlights the fit at higher temperatures. The approach of this curve to zero moment with decreasing temperature indicates that the coupling is antiferromagnetic. The asymptote of this curve at high temperatures corresponds to $\mu_{eff}^2 = 46$ (4), indistinguishable from the value for the uncoupled state of the dimer with $g = 1.96$ ($\mu_{eff}^2 = 46.1$).

Summary. The following are the principal findings and conclusions of this investigation. Results from a related study[3] are noted as appropriate.

(1) The binucleating ligand salmp forms a structurally analogous series of complexes $[M_2(salmp)_2]^{0,-,2-}$ with M = Fe and Mn, demonstrating that the trans-C_{2h} conformation can accommodate metal ions with high-spin octahedral radii of minimum range 0.78–0.97 Å. The distorted coordination units and the hydrolytic sensitivity of $[Mn_2(salmp)_2]^{2-}$ suggest that a (divalent) ion radius in excess of 1.0 Å may represent a size limit for a stable complex.

(2) The oxidation states $M^{II}M^{II}$, $M^{III}M^{II}$, and $M^{III}M^{III}$ can be isolated in stable compounds and are interconverted by (chemically) reversible electron-transfer reactions. The species $[Mn_2(salmp)_2]^{+,2+}$ can be generated electrochemically and likely contain the oxidation states $Mn^{IV}Mn^{III}$ and $Mn^{IV}Mn^{IV}$. The $[Mn_2(salmp)_2]^z$ electron-transfer series is one of the most extensive known for manganese. The existence of five detectable oxidation levels in the potential range $E_{1/2} \approx -0.4$ to +1.1 V (vs SCE) is due in part to the net charges of the complexes.

(3) $[Mn_2(salmp)_2]^{0,-,2-}$ is the only set of manganese complexes that are structurally characterized in three oxidation states with invariant terminal and bridging ligands. Jahn–Teller distortions are evident in $[Mn_2(salmp)_2]^{0,-}$. Both $[M_2(salmp)_2]^-$ species are valence-trapped in the solid and solution states from structural data and the appearance of intervalence charge-transfer bands. The two metal sites are structurally coupled.

(4) Whereas $[Fe_2(salmp)_2]^{0,-,2-}$ complexes are weakly ferromagnetic, and are the only examples of doubly bridged iron complexes with this property, $[Mn_2(salmp)_2]^{0,-,2-}$ complexes are weakly antiferromagnetic. For $Mn_2(salmp)_2$, $J = 6.5$ (2) cm^{-1} in $H_{ex} = JS_1 \cdot S_2$. Nearly all binuclear Mn^{III} complexes are antiferromagnetic,[11,15] and all species with the bridge unit $Mn^{III}(\mu\text{-}RO)_2Mn^{III}$ have this property.[24a,32b,37]

In ongoing work, we are analyzing in detail the EPR and Mössbauer spectroscopic and the bulk magnetic properties of the two series $[M_2(salmp)_2]^{0,-,2-}$ in order to achieve an internally self-consistent treatment of these properties for the three oxidation levels of M = Mn and Fe.[38] We are unaware of any other series of structurally defined compounds of these metals that provides this challenge. Last, we are cognizant of the possibility that these compounds might have value as structural and electronic models of non-oxo-bridged binuclear centers in proteins.

Acknowledgment. This research was supported by NIH Grant GM 28856. X-ray equipment was obtained through NIH Grant 1 S10 RR 02247. We thank S. C. Lee and M. J. Scott for useful discussions.

Supplementary Material Available: X-ray crystallographic data for the compounds in Table I, including tables of intensity collection data, complete positional and thermal parameters, bond distances and angles, and calculated hydrogen atom positions and ORTEP drawings (50 pages); tables of calculated and observed structure factors (72 pages). Ordering information is given on any current masthead page.

(37) (a) Torihara, N.; Mikuriya, M.; Okawa, H.; Kida, S. *Bull. Chem. Soc. Jpn.* **1980**, *53*, 1610. (b) Maslen, H. S.; Waters, T. N. *J. Chem. Soc., Chem. Commun.* **1973**, 760.

(38) Day, E. P.; Hendrich, M.; Holm, R. H.; Münck, E.; Snyder, B. S.; Wang, C.-P.; Yu, S.-B. Research in progress.